Hybrid Enzyme-Polymeric Capsules/Mesoporous Silica Nanodevice for In Situ Cytotoxic Agent Generation

Alejandro Baeza, Eduardo Guisasola, Almudena Torres-Pardo, José M. González-Calbet, Gustavo J. Melen, Manuel Ramirez, and Maria Vallet-Regí**

A novel nanocarrier based on functionalized mesoporous silica nanoparticles able to transport a non-toxic pro-drug and the enzyme responsible for its activation is presented. This nanodevice is able to generate in situ cytotoxic species once accumulated in the tumoral cell. Enzymes are sensitive macromolecules which can suffer denaturalization in biological media due to the presence of proteases or other aggressive agents. Moreover, the direct attachment of enzymes to the silica surface can reduce their activity by conformational changes or active site blockage. For these reasons, in order to create a robust system able to work in living organisms, the enzymes are previously coated with a protective polymeric shell which allows the attachment on the silica surface preserving their activity. The efficacy of this hybrid nanodevice for antitumoral purposes is tested against several human tumoral cells as neuroblastoma and leukemia showing significant efficacy. It converts this device in a promising candidate for further in vivo studies for oncology therapy.

1. Introduction

The development of novel nanodevices able to transport and release cytotoxic agents into tumoral tissues constitutes one of the most important field of the modern nanomedicine.[1] One of the main reasons for this interest is the fact that nanoparticles tend to be preferentially accumulated within tumoral tissues by a passive mechanism, called EPR effect (Enhance Permeation, and Retention).[2] This effect is based on the distinct blood vessel architecture present in solid tumors which is characterized by the presence of wide interendothelial junctions, large number of fenestrations and transendothelial pores with diameters as large as several hundred nanometers.[3] Thus, nanoparticles injected in the blood stream will pass through the fenestrations present in the tumoral vessels, while they are not able to cross through the healthy blood vessel walls.

In the recent years, a vast number of nanocarriers for drug delivery purposes have been described.[4] Among them, mesoporous silica particles are promising candidates due to their unique properties such as tuneable size, shape and porosity, high loading capacity, robustness and easy functionalization.[5] These characteristics provide unique opportunities to encapsulate different drugs, ranging from small molecules to therapeutic macromolecules.[6] In addition, their toxicity is low[7] showing good hemocompatibility, which is a must for intravenous administration.[8] The transport of highly toxic antitumoral drugs usually requires the development of carriers able to avoid the premature release of the loaded drugs before reaching the target, in order to avoid systemic toxicity.[9] This neccesity introduces high complexity in the synthesis of the carriers and therefore, it hampers the clinical application of these devices because their approval requires extensive safety evaluation of all the components.[10] In this work, we describe a simpler strategy based on the development of a novel nanocarrier capable to deliver a harmless prodrug into tumoral cells and once there, transform it into cytotoxic species which provoke the destruction of the malignat cell (**Figure 1**).

The most common strategy for the activation of prodrugs requires the presence of certain enzymes overexpressed in the target tissue.[11] However, this approach is limited in many cases by the scarce concentration of the activating enzyme into the target zone, which is not sufficient to generate enough amounts of drug necessary to provoke a significative response.[12] Moreover, there are many prodrugs for which the activating enzyme is not present. In this case, it is necesary to co-administrate the enzyme required for its activation or to introduce the gene required for its synthesis into the target cells.[13] Our system is based on a functionalized mesoporous silica nanoparticle loaded with a non-toxic prodrug, that is retained by electrostatic interactions within the porous silica network. The enzyme responsible for the drug activation is covalently anchored on the external surface. Indol-3-acetic acid (IAA) is a plant growth hormone which has been selected as pro-drug. It can be oxidized

Dr. A. Baeza, E. Guisasola, Prof. M. Vallet-Regí
Centro de Investigación Biomédica
en Red de Bioingeniería, Biomateriales
y Nanomedicina (CIBER-BBN)
Dpto. Química Inorgánica y Bioinorgánica
UCM, Instituto de Investigación Sanitaria Hospital,
12 de Octubre i+12., CEI Campus Moncloa,
UCM-UPM, Plaza Ramón y Cajal s/n 28040 Madrid, Spain
E-mail: abaezaga@ucm.es; vallet@ucm.es
Dr. A. Torres-Pardo, Prof. J. M. González-Calbet
Dpto. de Química Inorgánica
Facultad de Químicas
UCM, Madrid, Spain
Dr. G. J. Melen, Dr. M. Ramirez
Dpto. de Hematología y Oncología Pediátricas
del Hospital Infantil
Universitario Niño Jesús
Madrid, Spain

DOI: 10.1002/adfm.201400729

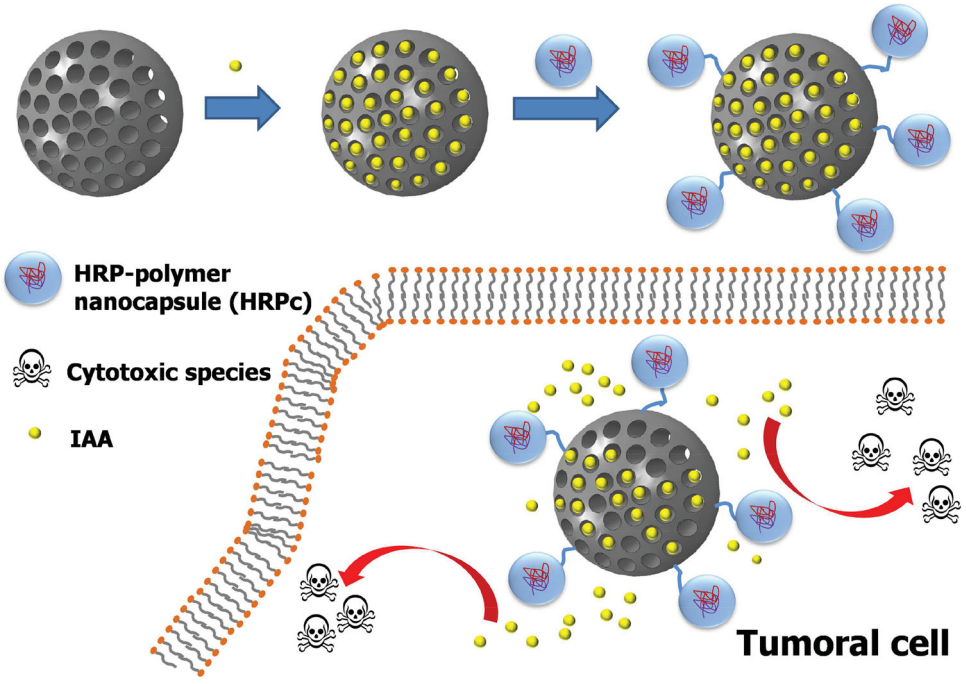

Figure 1. Schematic illustration of the in situ cytotoxic generation for antitumoral therapy.

by the enzyme horseradish peroxidase (HRP) producing cytotoxic compounds, mainly hydroxyl and reactive oxygen species (ROS), able to destroy human cancer cells by membrane and DNA damage.[14] IAA is not easily oxidized by mammalian peroxidases and, therefore, it is well tolerated in humans and even presents positive effects such as an increase in the phagocytic capacity of neutrophils[15] or antioxidant activity.[16] Therefore, the necessity to avoid the premature release of the housed pro-drug from the silica matrix is not as important as in the case of transporting conventional cytotoxic compounds. HRP also exhibits low toxicity in humans.

Direct attachment of enzymes on surfaces usually produces a significant reduction in their activity due to active site blockage or conformational changes during the process.[17] In addition, proteins usually present low stability in biological media due to the presence of proteases or other aggressive agents.[18] In order to overcome these limitations, the enzymes used in our device were previously coated with a polymeric capsule engineered to allow the grafting to the mesoporous surface and at the same time preserving their activity for longer times. Finally, the capacity of this novel nanocarrier to destroy human tumoral cells of neuroblastoma (NB1691-luc), a solid tumor which present a poor prognosis and B cell precursor leukemia (NALM-6), as a non-solid tumor model, was tested showing a significant efficacy.

2. Results and Discussion

2.1. Synthesis of Amine-Functionalized Mesoporous Silica Nanocarriers

In order to improve the loading and retention capacity of IAA within the pore network, mesoporous silica nanoparticles were synthesized in the presence of aminopropyltriethoxysilane (APTES) as functionalizing agent and tetraethylorthosilane (TEOS) as silica precursor, following a co-condensation method, which allows the production of homogeneously functionalized particles.[19] The presence of amino groups in the silica pore network is expected to improve the retention of IAA (pKa 4.75) at physiological pH, due to electrostatic interactions between the positively charged mesoporous particle surface with the anionic pro-drug. The maximal amount of functional groups which can be incorporated by a co-condensation method is limited by decrease of the mesoscopic order of the products and higher homocondensation reactions of the functionalized silica precursor with increasing the concentration.[19] In our case, three batches of particles were synthesized adding a mixture of APTES/TEOS, with different APTES proportion (10%, 20%, and 30% of APTES molar ratio). The particles as synthesized were called MSN-10N, MSN-20N, and MSN-30N respectively, according to the amount of APTES employed in the process. After the synthesis the surfactant was removed by ionic exchange using a solution of ammonium nitrate. The amount of amino groups was determined by thermal analysis being 5, 10, and 24% respectively which confirms the presence of a higher amount of amino groups on the silica surface and within the pore network when more APTES was added to the reaction media (Figure S1, Supporting Information). The size of each batch of particles was determined by dynamic light scattering (DLS) showing that the size distribution shifted to higher values (124 to 164 nm) when the concentration of APTES increased (**Figure 2**a). The average size of all batches was suitable for drug delivery applications in order to facilitate the cellular uptake.[20] The size distribution of each batch was confirmed by SEM and TEM (Figure 2c,d).

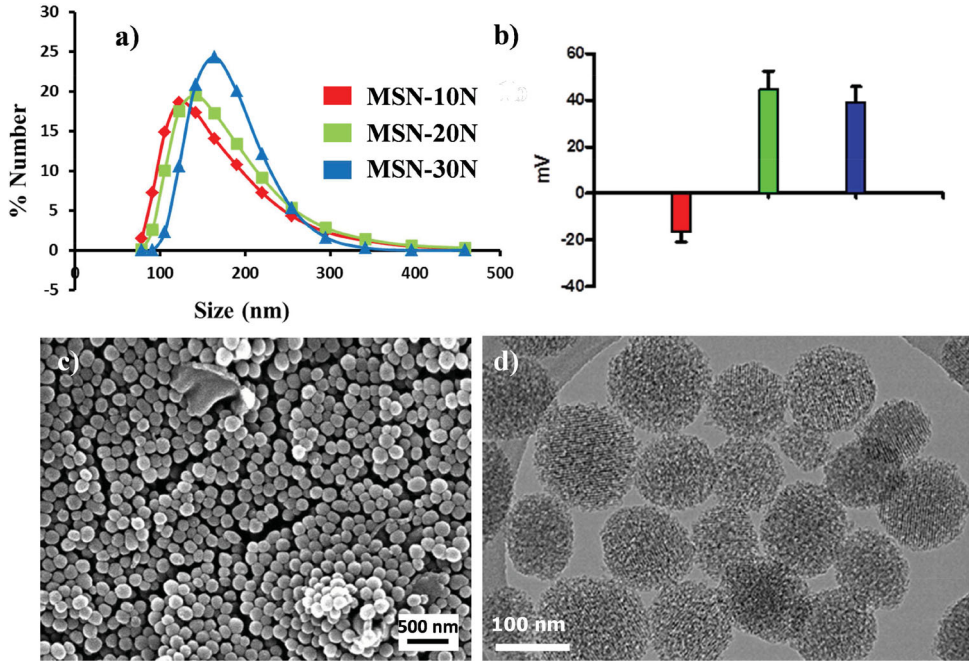

Figure 2. a) DLS and b) Z potential measurements of MSN materials. c,d) SEM and TEM images of MSN-30N (SEM and TEM images MSN-10N, 20N in Figure S2, Supporting Information).

Zeta potential measurements in water of these particles show drastic change on the superficial charge from –16 mV, in the case of MSN-10N, to +44 and +39 with MSN-20N and MSN-30N respectively (Figure 2b). Small-angle XRD pattern of the three batches show that the characteristic profile of MCM-41 materials is not affected by the use of higher amounts of APTES (Figure S3, Supporting Information). Nitrogen sorption isotherms indicate that the surface areas of these particles are comprised between 900–1200 $m^2\ g^{-1}$, with pore size distribution around 2.1–2.8 nm (Table S1, Supporting Information). Finally, the significant increase of the C–H (2900 cm^{-1}) and N–H (1520 cm^{-1}) bands in the FTIR spectra show that higher amounts of amino groups were incorporated when the concentration of APTES is augmented (Figure S4, Supporting Information).

2.2. IAA Release Profile of the Nanocarriers

In order to select the best material for IAA loading and release, the dried materials were soaked separately with IAA solution (25 mg mL^{-1}) in phosphate buffer (PB) pH 7.2 during 24 h. After that, the materials were filtered and the superficially adsorbed IAA was removed by washing with cold buffer. Then, a certain amount of each of the as loaded materials was suspended in fresh PB pH 7.2 on a Transwell permeable support of polycarbonate membrane. This membrane allows that small molecules (as IAA) can pass through its pores retaining the nanoparticles. Every hour, the liquid of each well was completely replaced by fresh buffer and the amount of IAA was determined by HPLC. The results indicate that MSN-30N is able to retain higher amounts of IAA, showing a loading capacity of 5% w/w, compared with MSN-20N and MSN-10N which present 2% and 0.25% w/w respectively (Figure S5, Supporting Information). Moreover, MSN-30N is able to maintain a sustained release of the prodrug during more time. For these reasons, this material was selected for further studies. It is worth to point out that these release experiments have been performed replacing totally the media with fresh buffer each hour which is better mimicking the real in vivo conditions.

2.3. Synthesis of HRP Nanocapsules

As it has been mentioned above, the aim of this work is to synthesize a material able to transport the pro-drug and the enzyme responsible for its activation simultaneously. Thus, this system can be able to generate enough amounts of cytotoxic agents once accumulated within the tumoral tissue by the EPR effect. However, the effective development of this strategy requires finding a suitable way to transport the enzyme through the body towards the tumoral mass, which is usually a great challenge. The presence of proteases and other aggressive agents both in the bloodstream and organ tissues can digest the proteins before they reach the target. Different approaches for transporting proteins have been described, from their encapsulation within nanoparticles[21] to the use of nanocarriers to transport the gene which encodes the protein into the target cells.[22] Recently, Lu et al. have described a novel methodology for protein delivery which consists in the synthesis of a polymer coating around the protein.[23] The resulting polymer-protein nanocapsule was stable against protease degradation and was able to be internalized by human cells.

In our work, we have applied a slightly modified method for the production of polymer-coated HRP nanocapsules with amino-functional groups on the external surface (**Scheme 1**).

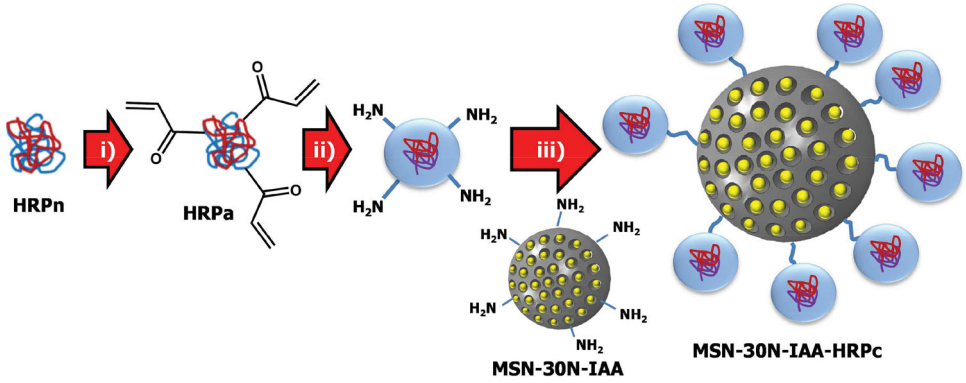

Scheme 1. Synthesis of the nanocarrier MSN-30N-IAA-HRPc. i) acrylic acid *N*-hydroxysuccinimide, ii) acrylamide: aminoethyl methacrylate hydrochloride: MBA (8:6.1), APS/TMEDA and iii) DSS.

These amino groups allow the further attachment of the enzyme nanocapsules to the mesoporous silica surface as is discussed below. The first step was the introduction of polymerizable acryloyl groups on the surface of the protein using acrylic acid *N*-hydroxysuccinimide ester in pH 8.5 Na_2CO_3 50 mM buffer, which reacts with the free amino groups present in the protein. The average amount of acryloyl groups introduced in each protein was determined by MALDI-TOF mass spectrometry resulting in approximately 4 groups per protein (Figure S6, Supporting Information). After that, the polymer shell was formed by radical polymerization using three different monomers: acrylamide, 2-aminoethyl methacrylate hydrochloride (which is responsible for the introduction of amino groups) and *N,N′*-methylene(bisacrylamide) as cross-linker, in molar ratio 8:6:1, respectively. The polymerization was initiated adding a solution of ammonium persulfate (APS) and *N,N,N′,N′*-tetramethylethylenediamine (TMEDA), yielding the protein-polymer capsule (HRPc) after 90 min at room temperature. The purification of both HRPa and HRPc was performed by centrifugation using centrifugal filters AMICON Ultra-2 30K and 50K respectively. It is important to note that both the acroylation and polymerization reactions were carried out in the presence of 4-dimethylaminoantipyrine (1:10 weight ratio to HRP) as stabilizer to prevent protein denaturalization.

DLS measurements in water indicated a significative increase in the hydrodynamic radius of the enzymes, from an average diameter of 4 nm to 8–9 nm, which clearly confirm the formation of the polymer coating (**Figure 3**a). This fact was confirmed

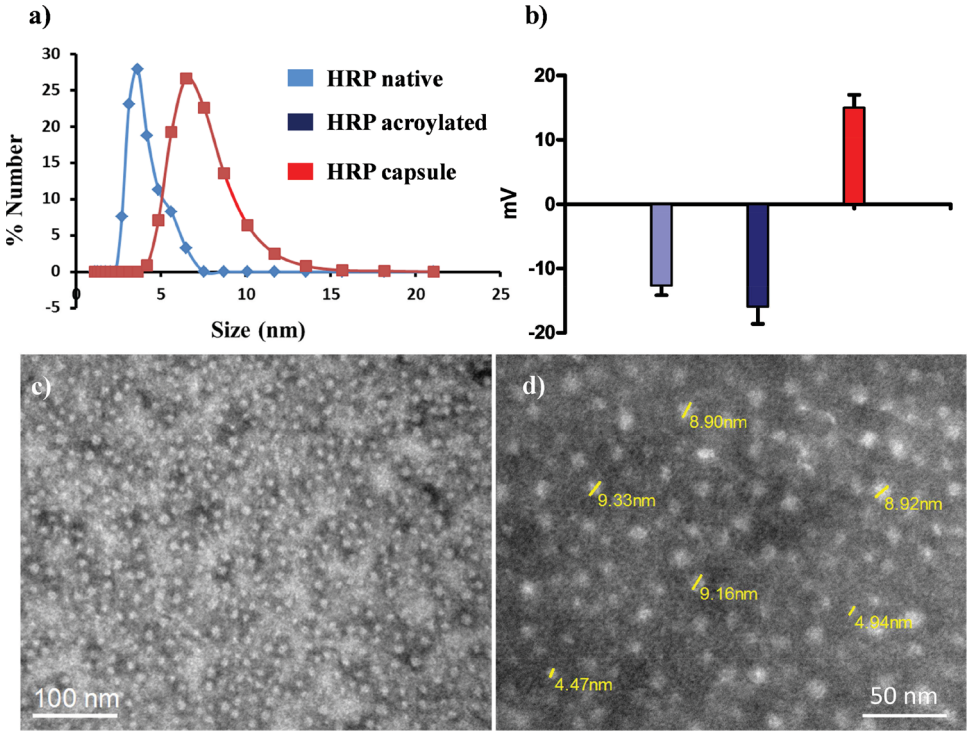

Figure 3. a) DLS and b) Zeta potential of HRP native, HRPa and HRPc, c-d) TEM of HRPc stained with phosphotungstic acid at different scales.

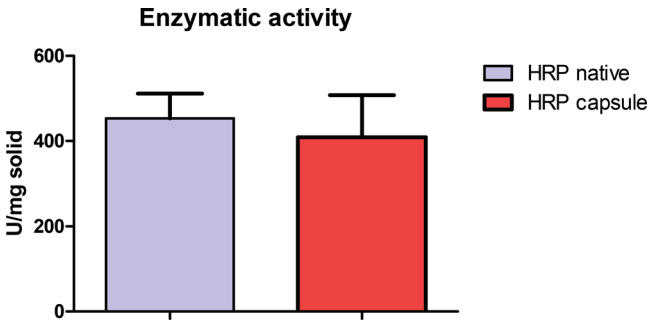

Figure 4. Enzymatic activity of HRP native and HRP capsule.

by TEM using phosphotungstic acid (PTA) as staining agent of the polymer shell. The capsules show an average diameter in accordance with the DLS measurements (Figure 3c,d). According to the zeta potential measurements in water, the acroylation process scarcely modified the surface charge of the native protein while a drastic change from negative to positive values is observed when the polymer shell is formed on the protein surface (Figure 3b). This result is consistent with the formation of a polymeric coating with free amino groups on the surface which are protonated at neutral pH.

In order to ascertain that the enzyme maintains its activity after the polymer coating, the enzymatic activity of the HRPc and the native precursor HRP were determined by the method developed by Trinder et al.[24] It follows the enzymatic oxidation of phenol by HRP in the presence of 4-aminoantipyrinie and hydrogen peroxide. Both activities were similar, which clearly indicates that the protein does not suffer significative alterations during the coating process (**Figure 4**). Moreover, HRPc solutions can be stored in the fridge for several weeks, without significant loss of activity which evidences that the polymeric shell preserves and protects the integrity of the biomolecule.

2.4. HRP Nanocapsule Attachment on Mesoporous Silica Surface

The attachment of the HRPc on the silica surface should be performed keeping inactive the enzyme during the process in order to avoid the premature conversion of the prodrug. Native HRP requires the presence of oxygen for the catalytic decomposition of IAA.[25] Thus, if oxygen is not present in the media or its concentration is low, the decomposition rate of IAA should be lower. In order to test this idea, a certain amount of HRPc (100 µg) was added to a solution of IAA in the presence or absence of oxygen (using nitrogen atmosphere and deoxygenated water). After 2 h, the amount of IAA was determined by HPLC indicating that if the reaction is carried out without oxygen, the concentration of IAA maintains almost equal to the initial (Figure S7, Supporting Information). Therefore, the grafting reaction of HRPc on the IAA-loaded particles was performed employing suberic acid bis(*N*-hydroxysuccinimide ester) (DSS) as amino-amino homofunctional cross-linker, keeping the reaction under nitrogen atmosphere and using buffers previously deoxygenated three times by freeze-pump-thraw cycles with N_2. The exact amount of HRPc anchored on the particle surface could not be precisely determined by TGA because the weight change before and after the grafting reaction is close to 1%. According to DLS measurements, the resulting system suffered an increase of around 20 nm in the diameter (**Figure 5**a) and a significative reduction of the zeta potential value, from +39 mV to +8 mV (data not shown) which indicates that the HRPc has been incorporated on the surface of the particles. The attached enzyme nanocapsules were clearly visible by TEM using phosphotungstic acid as staining agent (Figure 5b,c).

In order to be sure that the enzyme capsules attached on the mesoporous surface retain the activity after the grafting step, HRPc was also anchored on the surface of empty MSN-30N particles in the same conditions. The enzymatic activity

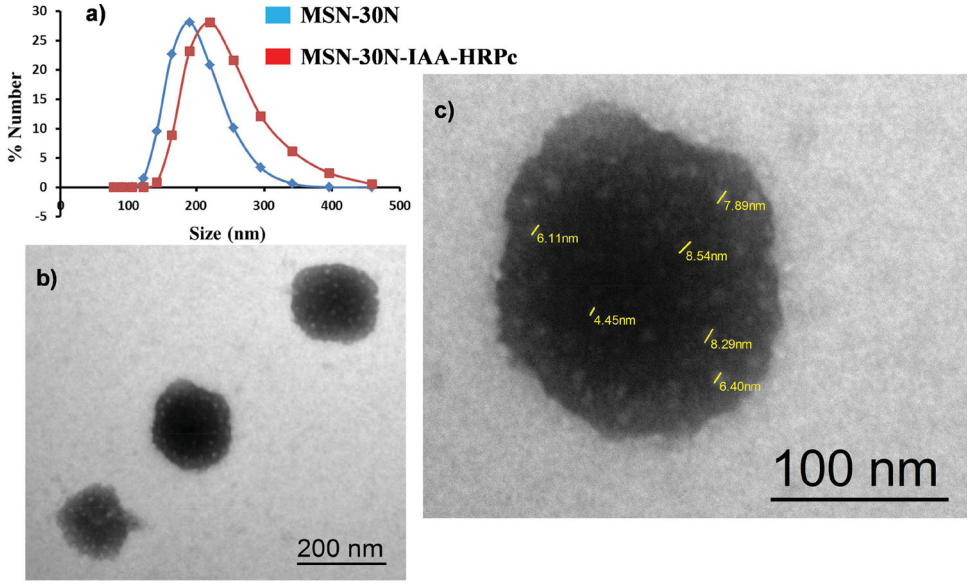

Figure 5. a) DLS measurements of MSN-30N and MSN-30N-IAA-HRPc. b,c) TEM of MSN-30N-IAA-HRPc stained with phosphotungstic acid.

of the resulting system was measured by the Trinder´s method, as in the previous case. The mesoporous nanoparticles functionalized with HRPc (MSN-30N-HRPc) showed an activity of 3–4 U g^{-1}, which is approximately one hundred times lower than the HRPc alone (≈400 U g^{-1}), which confirms that the grafting yield does not exceeds 1%. Moreover, this result indicates that HRPc can be covalently anchored on mesoporous particles retaining their activity (Figure S8, Supporting Information).

2.5. In Vitro Cytotoxicity and Cellular Uptake Evaluation

The antitumoral efficacy of this nanodevice was evaluated in vitro against two human tumoral cell lines, neuroblastoma (NB1691-luc) and leukemic (NALM6), due to the great importance of this type of tumours in pediatric oncology. The in vitro cytotoxicity study of the system was determined by the exposure of both cellular lines to increased amounts of nanomaterials in order to establish the minimal concentration required to induce significant cell mortality.

Cells were incubated for 4 h to allow the particle internalization, and then washed-out with PBS to remove the non-internalized particles and the prodrug released in the extracellular medium. Thus, only the effect provoked by the internalized particles will be tested. Then, cells were incubated overnight in fresh media. MSN-30N and MSN-30N-IAA were employed as controls. Cells incubated with the complete material (MSN-30N-IAA-HRPc) show rapidly decreasing viability at concentrations ranging from 0.1 to 0.5 mg mL^{-1} in both cases, whereas MSN-30N and MSN-30N-IAA only present a significant cell viability decrease in the case of leukemic cells when the concentration exceeds 1 mg mL^{-1} (**Figure 6**).

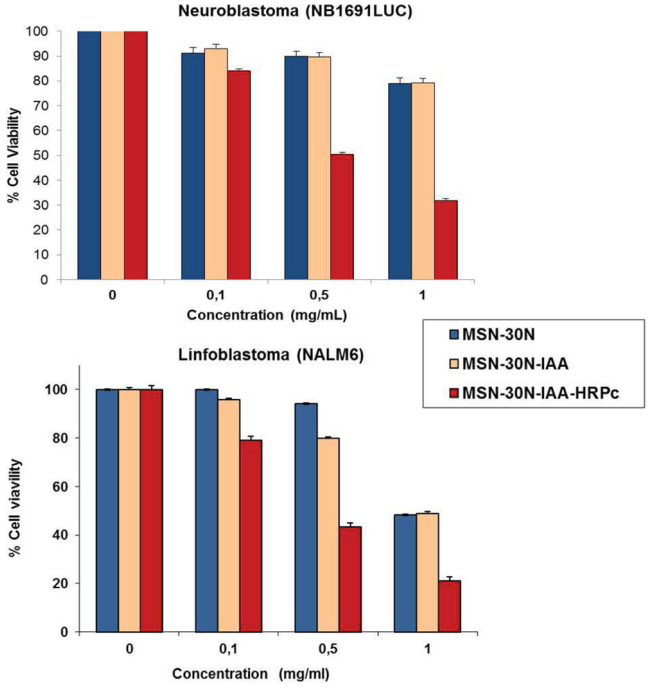

Figure 6. Cytotoxicity studies with neuroblastoma and leukemic cells.

The increased toxicity of the bare material in leukemic cells could be due to the fact that this cell line grows suspended in the media being more difficult to completely remove the non-internalized particles by washing steps after the incubation time.

Thus, the therapeutic window with the complete system (MSN-30N-IAA-HRPc) against these tumoral cell lines can be placed around 0.1–0.5 mg mL^{-1} where a high cell survival decrease is observed whereas the controls did not show any significant negative effect. It is interesting to note that higher concentration of free IAA, more than 5 mM, is required to kill neuroblastoma cells when they are incubated with a fixed concentration of HRPc (0.01 mg mL^{-1}). If the cells are treated with the native enzyme, no significative mortality was appreciated (Figure S9, Supporting Information). This result demonstrates that the encapsulation of IAA allows a better internalization within the cells improving its efficacy. Additionally, in order to be sure that the toxicity of the complete system was not due to the presence of the enzyme capsules, neuroblastoma cells were incubated with HRPc and native HRP, as controls, showing that both native enzyme and enzyme nanocapsule do not exhibit deleterious effects at the concentration present in the mesoporous materials and neither with higher amounts (Figure S10, Supporting Information).

To visualize the cellular uptake properties of these particles, a new batch of particles without IAA (MSN-30N) was labeled with rhodamine B isocyanate (RITC) whereas the enzyme capsules were labeled with fluorescein isocyanate (FITC). Then, the capsules were attached on the surface of the mesoporous particles following the same grafting procedure. Neuroblastoma cells were incubated in the presence of 0.5 mg/mL of these particles during four hours and after that time, the excess of non-internalized particles were removed by washing. The internalized particles were clearly observed by confocal fluorescence microscopy showing co-localization of both enzyme nanocapsules and mesoporous carriers, indicating that this nanodevice is able to pass through the cellular membrane (**Figure 7**).

3. Conclusions

In conclusion, a novel nanomaterial able to transport a non-toxic prodrug and the enzyme responsible for its conversion into cytotoxic compounds has been presented. This nanodevice can be internalized by tumoral cells and once there, it can generate enough amounts of cytotoxic species to destroy the diseased cells. This presents a novel way to treat tumors reducing the side effects of the current antitumoral therapy because it is based on the in situ generation of the cytotoxic compounds instead of transporting drugs in the activated state. The therapeutic efficacy of this system was evaluated in vitro against human tumoral cell lines (neuroblastoma and leukemia). The potential clinical application of these nanodevices requires extensive evaluation using animal models in order to determine their safety, pharmacokinetic and biodistribution. Further work is ongoing in order to test the efficacy of this device in neuroblastoma murine models.

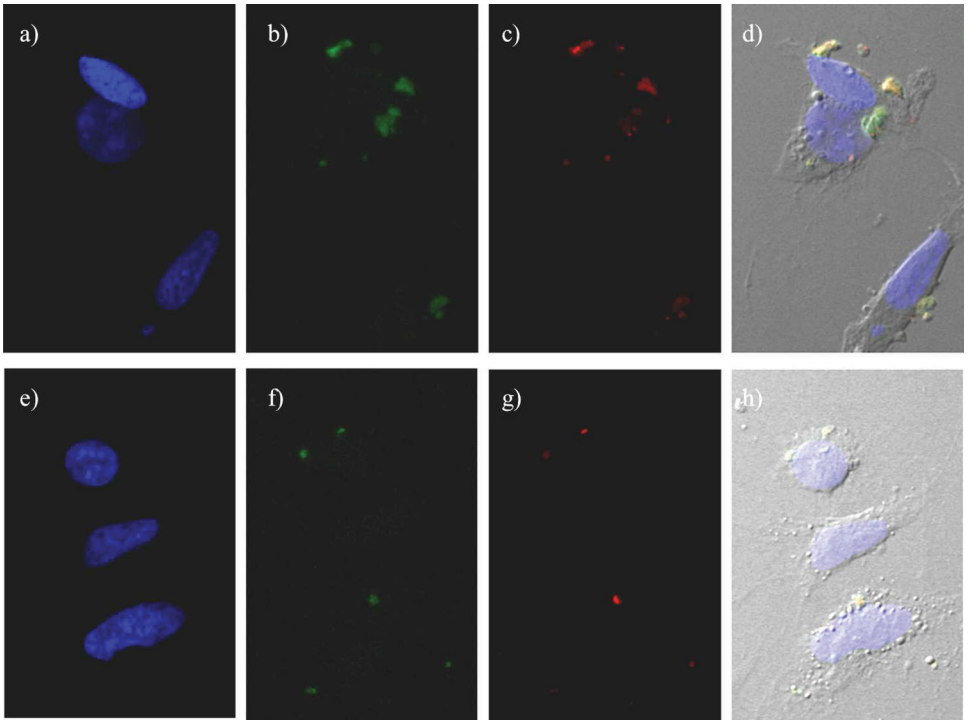

Figure 7. Representative confocal images of uptaked particles by neuroblastoma cells: a,e) cellular nucleus (stained with DAPI), b,f) FITC-enzyme capsules, c,g) RITC-mesoporous particles, and d,h) combined images with bright field

4. Experimental Section

Reagents: Following compounds were purchased from Sigma-Aldrich Inc.: Peroxidase from horseradish (HRP) (powder, 250–300 U mg^{-1} solid using pyrogallol), indol-3-acetic acid sodium salt, suberic acid bis(N-hydroxysuccinimide ester) (DSS), acrylic acid *N*-hydroxysuccinimide ester, 2-aminoethyl methacrylate hydrochloride, acrylamide, 4-dimethylaminoantipyrine, *N*,*N*′-methylene(bisacrylamide) (MBA), aminopropyltriethoxysilane (APTES), ammonium persulfate (APS), ammonium nitrate, cetyltrimethylammonium bromide (CTAB), tetraethyl orthosilicate (TEOS) and *N*,*N*,*N*′,*N*′-Tetramethylethylenediamine (TMEDA), rhodamine b and fluorescein isothiocyanate. These compounds were used without further purification. Deionized water was purified by passage through a Milli-Q Advantage A-10 Purification System (Millipore Corporation) to a final resistivity of 18.2 MΩ cm. Acroylated HRP and HRP capsules were purified by ultrafiltration using centrifugal filter devices (AMICON Ultra-2 30K and 50K). All other chemicals (absolute ethanol, acetone, etc.) were of the best quality commercially available and they have been employed as received.

Characterization Techniques: Powder X-ray diffraction (XRD) experiments were performed with a Philips X'Pert diffractometer equipped with Cu Kα radiation (wavelength 1.5406 Å). XRD patterns were collected in the 2θ range between 0.6° and 8 with a step size of 0.02° and counting time of 5 s per step. Fourier transform infrared spectroscopy (FTIR) in a Thermo Nicolet nexus equipped with a Goldengate attenuated total reflectance device. The textural properties of the materials were determined by nitrogen sorption porosimetry by using a Micromeritics ASAP 2020. To perform the N_2 measurements, the samples were previously degassed under vacuum for 24 h at room temperature. Thermogravimetry analysis (TGA) were performed in a Perkin Elmer Pyris Diamond TG/DTA analyzer, with 5 °C min^{-1} heating ramps, from room temperature to 600 °C. The hydrodynamic size of mesoporous nanoparticles and protein capsules was measured by means of a Zetasizer Nano ZS (Malvern Instruments) equipped with a 633 nm "red" laser. Mass spectra were acquired with a Voyager DE-STR Biospectrometry MALDI-TOF mass spectrometer. Transmission electron microscopy (TEM) was carried out with a JEOL JEM 1010 and JEOL JEM 2100 instruments operated at 100 kV and 200 kV, equipped with a CCD camera (KeenView Camera). Sample preparation was performed by dispersing in distilled water and subsequent deposition onto carbon-coated copper grids. A solution of 1% of phosphotungstic acid (PTA) pH 7.0 was employed as staining agent in order to visualize the protein capsules alone and attached on the mesoporous surface. Scanning electron microscopy (SEM) analyses were made on a JEOL 6400-LINK AN10000 microscope (Electron Microscopy Centre, UCM). The samples underwent Au metallization previous to observation.

Calculation Procedures: The surface area was determined using the Brunauer-Emmett-Teller (BET) method and the pore volume, Vpore (cm^3 g^{-1}), was estimated from the amount of N_2 adsorbed at a relative pressure around 0.99. The pore size distribution between 0.5 and 40 nm was calculated from the desorption branch of the isotherm by means of the Barrett-Joyner-Halenda (BJH) method. The mesopore size, Øpore (nm), was determined from the maximum of the pore size distribution curve.

Synthesis of Amino-Functionalized Mesoporous Silica Nanoparticles (MSN-XXN): Three different batches of mesoporous silica nanoparticles (MSNs) were synthesized according with the proportion of APTES in relation with TEOS employed in the process. The general method was as following: to a 500 mL round-bottom flask, 0.5 g of CTAB as a structure-directing agent, 240 mL of H_2O (Milli-Q), 1.75 mL of NaOH (2 M) was added. The mixture was heated to 80 °C and stirred at 600 rpm. When the reaction mixture was stabilized at 80 °C, 12.2 mmol of a mixture of APTES/TEOS (10%, 20%, or 30% APTES molar ratio, respectively) was added dropwise at 0.25 mL min^{-1} rate. The white suspension obtained was stirred during further 2h at 80 °C. The reaction mixture was filtered and washed with 50 mL of H_2O, and then three more times with 50 mL of EtOH. Finally, the surfactant was removed by ionic exchange using a solution of amonium nitrate (10 mg mL^{-1}) in 175 mL of ethanol (95%) at 65 °C overnight under magnetic stirring. The process was repeated three times. Samples were named as MSN-10N, MSN-20N, or MSN-30N according with the amount of employed APTES.

Loading IAA in MSN-XXN: 25 mg of MMSN-XXN were placed in a three-neck round bottom flask and dried at 80 °C under vacuum for 24 h. Then, 2 mL of IAA aqueous solution (25 mg mL^{-1}) were added and the suspension was stirred at room temperature for 24 h. After that time, the sample was filtered and washed smoothly two times with cold water (2 mL × 2 mL) in order to remove the IAA absorbed on the external surface. Finally, the products were dried under vacuum at 25 °C.

Release of IAA from MSN-XXN: 5 mg of IAA-loaded MSN-XXN were suspended in 0.5 mL of fresh PB pH 7.2 (100 mM) and placed on a Transwell permeable support with 0.4 μm of polycarbonate membrane. The well was filled with 1.0 mL of PB pH 7.2 (100 mM) and the suspension was stirred at 150 rpm during all the experiment. Every hour, the amount of IAA was determined using a Waters 2695 HPLC separation module combined with a PDA detector and then, the media was replaced by other 1.0 mL of fresh buffer. The employed column was an XTerra RP18 4.6 mm × 150 mm (Waters) containing 5 μm of C18 silica beads, using injected volumes of 10 μL. The mobile phase was isocratic elution with 40:60% (A:B) of acetonitrile:H_2O (75/25 v/v) (A) and NaOAc 20 mM (B) at 30 °C and flow rate of 0.5 mL min^{-1}. Under these conditions the retention time of the IAA was 3.0–3.20 min. Detection was performed by UV at 280 nm and chromatograms were recorded on an Endpower-2 integrator.

Synthesis of Acroylated HRPa: 5 mg of HRP and 0.5 mg of 4-dimethylaminoantipyrine were dissolved in 1.8 mL of pH 8.5 Na_2CO_3 (50 mM) at room temperature. To this solution, 2 mg of acrylic acid *N*-hydroxysuccinimide ester dissolved in 20 μL of DMSO were added. The solution was stirred for 2 h. The protein was purified by centrifugal separation with 30 KDa cut-off filters (AMICON Ultra-2 30K) and washed three times with fresh pH 8.5 Na_2CO_3 (50 mM) buffer. The protein was concentrated to final volume of 200 μL.

Synthesis of HRP Capsule (HRPc): All of the acroylated protein solution obtained before was diluted with 2.8 mL of pH 8.5 Na_2CO_3 (50 mM) buffer previously deoxygenated three times by freeze-pump-thraw cycles with N_2. To this solution, a mixture of 8.5 mg of acrylamide, 15 mg of 2-aminoethyl methacrylate hydrochloride, 2.3 mg of *N*,*N*′-methylene(bisacrylamide) and 0.5 mg of 4-dimethylaminoantipyrine dissolved in 2 mL of deoxygenated pH 8.5 Na_2CO_3 (50 mM) buffer was added. The reaction media was placed in an orbital stirrer at 150 rpm for 10 min. After this time, 5 mg of ammonium persulfate (APS) and 5 μL of TMEDA dissolved in 30 μL of DMSO was added. The reaction mixture was stirred at 150 rpm during 90 min at room temperature. The protein capsule was purified by centrifugal separation with 50 KDa cut-off filters (AMICON Ultra-2 50K) and washed three times with pH 7.2 PB (100 mM) buffer. The protein was concentrated to final volume of 500 μL.

Attachment of HRPc on the MSN-30N Surface: 2 mg of suberic acid bis(N-hydroxysuccinimide ester) dissolved in 50 μL of DMSO were added to a solution of 1 mg of HRPc in 1 mL of deoxygenated pH 7.2 PB (100 mM) buffer. The reaction mixture was placed in an orbital stirrer at 150 rpm at room temperature under nitrogen atmosphere during 30 min. After this time, the solution was filtered using a nylon membrane of 0.45 μm in order to remove the unreacted DSS and other salts precipitated in the water solution and the resulting liquid was added over a suspension of 20 mg of MSN-30N-IAA in 1 mL of deoxygenated pH 7.2 PB (100 mM) buffer. The mixture was stirred during 2 h under nitrogen atmosphere. The particles were filtered and washed smoothly two times with cold water, in order to remove the non-attached HRPc, and dried under N_2 flux at room temperature.

Cytotoxicity of the Enzymes (HRP Native and HRPc): The study of the cytotoxicity of HRP native and HRPc in the presence of increasing concentrations of enzyme was performed using the neuroblastoma cell line (NB1691-luc). Cells were seeded in 48-well plates at a density of 5000 cells cm^{-2}. Cells were exposed to different concentrations of HRP or HRPc during 4 h at 37 °C, and 5% CO_2. After that time, cells were washed and remained in culture for other 14 h. Finally, cells were harvested and cell viability was determined by flow cytometry with 7AAD (Biolegends, San Diego, CA.) using the FACSCanto II flow cytometer and the FACSDiva software v6.1.2 (BD Biosciencies, San Jose, Ca.)

Cytotoxicity of Enzymes (HRP Native and HRPc) Using Increased Concentrations of IAA: This study was performed using the neuroblastoma cell line (NB1691-luc). Cells were seeded in 48-well plates at a density of 5000 cells cm^{-2}. Cells were exposed to different concentrations of IAA with a fixed concentration of enzyme of 0.01 mg mL^{-1} (HRP native or HRPc, respectively) during 4 h at 37 °C, and 5% CO_2. After that time, cells were washed and remained in culture for other 14 h. Finally, cells were harvested and cell viability was determined by flow cytometry with 7AAD (Biolegends, San Diego, CA.) using the FACSCanto II flow cytometer and the FACSDiva software v6.1.2 (BD Biosciencies, San Jose, Ca.)

Cytotoxicity of the Mesoporous Silica Devices (MSN-30N, MSN-30N-IAA and MSN-30N-IAA-HRPc): In the case of the cytotoxic evaluation of the complete system, the studies were performed using the neuroblastoma cell line (NB1691-luc) and lymphoblastic NALM6 cell lines. Cells were seeded in 48-well plates at a density of 5000 cells cm^{-2}. Cells were exposed to different concentrations of MSN-30N, MSN-30N-IAA and MSN-30N-IAA-HRPc during 4 h at 37 °C, and 5% CO_2. After that time, cells were washed and remained in culture for other 14 h. The viability assay was carried out as the previous case. Results are shown as the mean of two independent replicates.

Synthesis of MSN-30N Labeled with RITC: 1 mg of rhodamine B isocyanate dissolved in 40 μL of DMSO was added to a suspension of 100 mg of MSN-30N particles in 2 mL of Milli-Q water. The suspension was stirred at 200 rpm at room temperature during 12 h. The particles were washed three times with water and dried overnight in a vacuum oven at 30 °C.

Synthesis of HRPc-FITC: 0.5 mg of FITC dissolved in 40 μL of DMSO were added to a solution of 5 mg of HRPa in 2 mL of pH 8.5 Na_2CO_3 (50 mM) buffer. The suspension was placed in an orbital stirred at 100 rpm and room temperature during 1 h. After that time, the protein capsule was purified by centrifugal separation with 50KDa cut-off filters (AMICON Ultra-2 50K) and washed three times with pH 7.2 PB (100 mM) buffer. The polymer capsule with the fluorescein labeled proteins and their attachment on the rhodamine B labeled mesoporous particles were performed following the similar procedures that are described above. The particles were dried by N_2 flux at room temperature. The particles were called MSN-30N-HRPc-F-R.

Internalization Studies by Confocal Fluorescence Microscopy: NB1691Luc cells were seeded on glass chamber slides (LabTek II, Nunc, Rochester, NY) and incubated with 0.5 mg mL^{-1} MSN-30N-HRPc-F-R for 4 hours. Internalization was stopped by washing cells with ice-cold PBS followed by two acid washes with 250 mM NaCl, 100 mM glycine pH 2.5 to remove any adsorbed particules. Cells were then fixed with 4% PFA and mounted with DAPI-containing Fluoroshield (Sigma, St. Louis, MO). Images were capture with the Leica SP5 confocal microscope and the Leica LAS AF software.

Supporting Information

Supporting Information is available from the Wiley Online Library or from the author.

Acknowledgements

This work was supported by the Ministerio de Economía y Competitividad, through project MAT2011–15138-E, Spanish CICYT through project MAT-2008–00736, and Spanish National CAM through project S2009/MAT-172. E.G. and A.T.P. thanks CEI Campus Moncloa for the PICATA fellowship. The authors also thank the X-ray Diffraction C.A.I. and the National Electron Microscopy Center, UCM.

Received: March 4, 2014
Published online: April 22, 2014

[1] a) I. Brigger, C. Dubernet, P. Couvreur, *Adv. Drug Delivery Rev.* **2012**, *64*, 24–36; b) A. Schroeder, D. A. Heller, M. M. Winslow, J. E. Dahlman, G. W. Pratt, R. Langer, T. Jacks, D. G. Anderson, *Nat. Rev. Cancer* **2012**, *12*, 39–50; c) A. H. Faraji, P. Wipf, *Bioorg. Med. Chem.* **2009**, *17*, 2950–2962.
[2] H. Maeda, H. Nakamura, J. Fang, *Adv. Drug Delivery Rev.* **2013**, *65*, 71–79.
[3] R. K. Jain, T. Stylianopoulos, *Nat. Rev: Clin. Oncol.* **2010**, *7*, 653–664.
[4] a) J. H. Adair, M. P. Parette, E. I. Altinoglu, M. Kester, *ACS Nano* **2010**, *4*, 4967–4970; b) W. B. Liechty, N. A. Peppas, *Eur. J. Pharm. Biopharm.* **2012**, *80*, 241–246; c) F. M. Kievit, M. Zhang, *Acc. Chem. Res.* **2011**, *44*, 853–862; d) M. Colilla, B. González, M. Vallet-Regí, *Biomater. Sci.* **2013**, *1*, 114–134.
[5] a) F. Tang, L. Li, D. Chen, *Adv. Mater.* **2012**, *24*, 1504–1534; b) M. Vallet-Regí, M. Manzano, M. Colilla, in *Biomedical applications of mesoporous ceramics*, CRC Press, Boca Ratón, FL **2013**; c) J. Simmchem, A. Baeza, D. Ruiz-Molina, M. J. Esplandiu-Egido, M. Vallet-Regí, *Small* **2012**, *8*, 2053–2059.
[6] a) M. Vallet-Regí, E. Ruiz-Hernández, *Adv. Mater.* **2011**, *23*, 5177–5218; b) M. Vallet-Regí, E. Ruiz-Hernández, B. González, A. Baeza, *J. Biomat. Tissue Eng.* **2011**, *1*, 6–29; c) Z. Li, J. C. Barnes, A. Bosoy, J. F. Stoddart, J. I. Zink, *Chem. Soc. Rev.* **2012**, *41*, 2590–2605; d) V. Mamaeva, C. Sahlgren, M. Lindén, *Adv. Drug Delivery Rev.* **2013**, *65*, 689–702.
[7] J. Lu, M. Liong, Z. Li, J. I. Zink, F. Tamanoi, *Small* **2010**, *6*, 1794–1805.
[8] Y. Zhao, X. Sun, G. Zang, B. G. Trewyn, I. I. Slowing, V. S-Y. Lin, *ACS Nano* **2011**, *5*, 1366–1375.
[9] a) A. Baeza, E. Guisasola, E. Ruiz-Hernández, M. Vallet-Regí, *Chem. Mater.* **2012**, *24*, 517–524; b) E. Ruiz-Hernández, A. Baeza, M. Vallet-Regí, *ACS Nano* **2011**, *5*, 1259–1266.
[10] V. J. Venditto, F. C. SzokaJr, *Adv. Drug Delivery Rev.* **2013**, *65*, 80–88.
[11] a) A. Popat, B. P. Ross, J. Liu, S. Jambhrunkar, F. Kleitz, S. Z. Qiao, *Angew. Chem. Int. Ed.* **2012**, *51*, 12486–12489; b) D. Niculescu-Duvaz, G. Negoita-Giras, I. Niculescu-Duvaz, D. Hedley, C. J. Springer, in *Prodrugs and Targeted Delivery: Towards Better ADME Properties*, (Ed: Jarkko Rautio) Wiley-VCH, Weinheim, **2011**, pp 271–344.
[12] J. Rautio, H. Kumpulainen, T. Heimbach, R. Oliyai, D. Oh, T. Järvinen, J. Savolainen, *Nat. Rev. Drug Discovery* **2008**, *7*, 255–270.
[13] M. Rooseboom, J. N. N. Commandeur, N. P. E. Vermeulen, *Pharmacol. Rev.* **2004**, *56*, 53–102.
[14] a) D. S. Kim, S. E. Jeon, K. C. Park, *Cell. Signal.* **2004**, *16*, 81–88; b) M. P. de Melo, T. M. de Lima, T. C. Pithon-Curi, R. Curi, *Toxicol. Lett.* **2004**, *148*, 103–111.
[15] S. M. P. Pugine, P. Brito, T. C. Alba-Loureiro, E. J. X. Costa, R. Curi, M. P. de Melo, *Cell Biochem. Funct.* **2007**, *25*, 723–730.
[16] L. R. B. Mourão, R. S. S. Santana, L. M. Paulo, S. M. P. Pugine, L. M. Chaible, H. Fukumasu, M. L. Z. Dagli, M. P. de Melo, *Cell Biochem. Funct.* **2009**, *27*, 16–22.
[17] C. Mateo, J. M. Palomo, G. Fernandez-Lorente, J. M. Guisan, R. Fernandez-Lafuente, *Enz. Microbial Technol.* **2007**, *40*, 1451–1463.
[18] C. O. Fagain, *Biochim. Biophys. Acta* **1995**, *1252*, 1–14.
[19] F. Hoffmann, M. Cornelius, J. Morell, M. Fröba, *Angew. Chem. Int. Ed.* **2006**, *45*, 3216–3251.
[20] F. Lu, S-H. Wu, Y. Hung, C-Y. Mou, *Small* **2009**, *5*, 1408–1413.
[21] a) I. I. Slowing, B. G. Trewyn, V. S-Y. Lin, *J. Am. Chem. Soc.* **2007**, *129*, 8845–8849; b) A. Vila, A. Sánchez, M. Tobío, P. Calvo, M. J. Alonso, *J. Controlled Release* **2002**, *78*, 15–24.
[22] a) O. Greco, S. Rossiter, C. Kanthou, L. K. Folkes, P. Wardman, G. M. Tozer, G. U. Dachs, *Mol. Cancer Ther.* **2001**, *1*, 151–160; b) I. Niculescu-Duvaz, R. Spooner, R. Marais, C. J. Springer, *Bioconjugate Chem.* **1998**, *9*, 4–22.
[23] a) Y. Liu, J. Du, M. Yan, M. Y. Lau, J. Hu, H. Han, O. O. Yang, S. Liang, W. Wei, H. Wang, J. Li, X. Zhu, L. Shi, W. Chen, C. Ji, Y. Lu, *Nat. Nanotechnol.* **2013**, *8*, 187–192; b) M. Yan, J. Du, Z. Gu, M. Liang, Y. Hu, W. Zhang, S. Priceman, L. Wu, Z. H. Zhou, Z. Liu, T. Segura, Y. Tang, Y. Lu, *Nat. Nanotechnol.* **2010**, *5*, 48–53.
[24] P. Trinder, D. Webster, *Ann. Clin. Biochem.* **1984**, *21*, 430–433.
[25] L. K. Folkes, P. Wardman, *Biochem. Pharmacol.* **2001**, *61*, 129–136.